# Conditions and Possibilities for Rare-Earth Doping of $KTiOPO_4$ Flux-Grown Single Crystals

R. Solé,[†] V. Nikolov,[‡] I. Koseva,[‡] P. Peshev,[‡] X. Ruiz,[†] C. Zaldo,[§] M. J. Martín,[§] M. Aguiló,[†] and F. Díaz*,[†]

*Laboratori de Física Aplicada i Cristal.lografia. Universitat Rovira i Virgili, 43005 Tarragona, Spain; Institute of General and Inorganic Chemistry, Bulgarian Academy of Sciences, 1113 Sofia, Bulgaria; and Instituto de Ciencia de Materiales de Madrid, Consejo Superior de Investigaciones Científicas, Cantoblanco, 28049 Madrid, Spain*

*Received December 19, 1996. Revised Manuscript Received August 8, 1997*[⊗]

The growth of rare-earth (RE = Nd, Tb, Ho, Er, Tm, and Yb) doped $KTiOPO_4$ (KTP) single crystals from high-temperature solutions [$K_2O-P_2O_5-TiO_2-RE_2O_3$ (or $Tb_4O_7$)] was investigated. The concentration regions of crystallization of RE-doped KTP, the maximum (critical) RE concentrations in the solution without losing the KTP phase and the corresponding upper limit of RE ions incorporated into the KTP lattice were obtained experimentally. The crystallization regions of RE-doped KTP are significantly narrower than the region of undoped KTP. Above a certain critical RE concentration in the solution, RE phosphate phases crystallize. The highest concentration of RE in the crystal is in the range 50−600 ppm and strongly depends on the RE ionic radius. Some double substitutions with Nd and a codopant element can significantly change this concentration. In addition, RE-doped KTP single crystals were grown by the top seeded solution growth (TSSG) technique, and their experimental conditions were compared with those of undoped KTP single-crystal growth. Optical absorption spectra for Ho-, Er-, and Tm-doped KTP were obtained and discussed.

## Introduction

Potassium titanyl phosphate ($KTiOPO_4$, hereafter KTP), together with many of its structural analogues, is one of the most attractive materials for nonlinear optical (NLO) and electrooptical applications because it has good NLO properties and a high laser damage threshold and it is chemically stable.[1,2]

In recent years, different investigations have been carried out to improve the properties of the KTP single crystals and to find new applications for them. Most of these investigations are related to doped KTP materials. For instance, the ionic conductivity in the *c* direction of flux-grown KTP, which is relatively high for some electrooptical applications, can be reduced significantly if $Me^{3+}$ (Al, Ga, Cr) is used as dopant with a concentration of about 500−1000 ppm.[3−5] Doping may also influence the matching conditions for second harmonic generation (SHG). The transparency of KTP ranges from 350 to 4500 nm, but the small birefringence of KTP does not allow noncritical type II phase matching below 990 nm cutoff wavelength for the fundamental radiation. The reduction of this KTP cutoff wavelength is required to produce compact solid-state blue lasers by frequency-doubling diode emissions. This can be achieved by modifying the KTP birefringence by doping.[6] Up to 100 nm of cutoff wavelength, reduction has been obtained by doping with Nb.[6] With the same aim, Anderson et al.[7,8] have investigated transition-metal-doped KTP and Er- or Yb-doped $RbTiOAsO_4$ powders. Rare-earth ions have absorption bands in the visible region that lie between the fundamental and second harmonic of Nd:YAG laser radiation. They claim that this gives anomalous dispersion and induces an SHG effect at wavelengths shorter than 990 nm.

Rare-earth ions in KTP or in its isomorphs may influence the properties in the areas mentioned above since they have lower ionic charges than $Ti^{4+}$ (to reduce the ionic conductivity[9]) and specific absorption bands in the near-ultraviolet and visible regions (to provide an anomalous dispersion[7,8]). In addition, a self-doubling output could be obtained if a NLO material, such as KTP, was doped with $RE^{3+}$ elements. For an accurate determination of some physical properties of KTP such as SHG, ionic conductivity, optical absorption, or luminescence spectra, inclusion-free single crystals of the desired size are preferable.

The aim of this work was to investigate the possibilities for doping KTP with different rare earth elements, as well as the conditions of growth inclusion-free RE-doped single crystals by the top seeded solution growth (TSSG) technique. In addition, a summary of results about the optical properties of RE-doped KTP is presented.

* To whom correspondence should be addressed.
[†] Universitat Rovira i Virgili.
[‡] Bulgarian Academy of Sciences.
[§] Instituto de Ciencia de Materiales de Madrid.
[⊗] Abstract published in *Advance ACS Abstracts,* November 15, 1997.
(1) Liu Y. S.; Deutz D.; Belt R. *Opt. Lett.* **1984**, *9*, 76.
(2) Bierlein, J. D.; Vanherzeele, H. *J. Opt. Soc. Am.* **1989**, *B6*, 622.
(3) McGee, T. F.; Blom, G. M.; Kostecky, G. *J. Cryst. Growth* **1991**, *109*, 361.
(4) Bolt, R. J. *J. Cryst. Growth* **1993**, *126*, 175.
(5) Hörlin, T.; Bolt, R. *Solid State Ionics* **1995**, *78*, 55.
(6) Cheng, L. T.; Cheng, L. K.; Harlow R. L.; Bierlein, J. D. *Appl. Phys. Lett.* **1994**, *64*, 155.
(7) Anderson, M. T.; Phillips, M. L. F.; Stucky G. D. *J. Non-Cryst. Solids* **1994**, *178*, 120.
(8) Anderson, M. T.; Phillips, M. L. F.; Sinclair, M. B.; Stucky G. D. *Chem. Mater.* **1996**, *8*, 248.
(9) Nikolov, V.; Koseva, I.; Peshev, P.; Solans, X.; Solé, R.; Ruiz, X.; Gavaldà, Jna.; Aguiló, M.; Diaz, F. *J. Cryst. Growth*, submitted.

S0897-4756(96)00644-8 CCC: $14.00 

**Table 1. Several Data Associated with RE Doping in KTP[a]**

| | A | B | C | D | E | F | G |
|---|---|---|---|---|---|---|---|
| | undoped | | | | | | 865.05 |
| I | Nd | 0.983 [6] | 6 | 6 | 52 | $0.6 \times 10^{-3}$ | 866.74 |
| | Tb | 0.923 [6] | 3 (as $Tb_4O_7$) | 3 | 203 | $2.2 \times 10^{-3}$ | 862.43 |
| | Ho | 0.901 [6] | 8 | 8 | 342 | $2.7 \times 10^{-3}$ | 869.30 |
| | Er | 0.890 [6] | 5.5 | 5.5 | 330 | $3.8 \times 10^{-3}$ | 866.00 |
| | Tm | 0.880 [6] | 6.5 | 6 | 503 | $5.1 \times 10^{-3}$ | 868.94 |
| | Yb | 0.861 [6] | 6 | 6 | 581 | $5.8 \times 10^{-3}$ | 869.47 |
| II | $Nd^{3+} + Al^{3+}$ | 0.537 [6] | 4.5 + 4.5 | 4 + 4 | 69/240 | $1.0 \times 10^{-3}/1.8 \times 10^{-2}$ | 863.00 |
| | $Nd^{3+} + Nb^{5+}$ | 0.640 [6] | 1 + 1 | 1 + 1 | 53/7291 | $3.5 \times 10^{-3}/7.6 \times 10^{-1}$ | 869.28 |
| III | $Nd^{3+} + Rb^{+}$ | 1.610 [8] | 4.5 + 4.5 | 4 + 4 | 138/18317 | $2.0 \times 10^{-3}/1.5 \times 10^{-1}$ | 867.93 |
| | $Nd^{3+} + Na^{+}$ | 1.180 [8] | 5.5 + 5.5 | 5 + 5 | 26/1390 | $0.3 \times 10^{-3}/3.7 \times 10^{-2}$ | 866.46 |
| IV | Nd + Si | 1.64* [4] | 3 + 3 | 3 + 3 | 53/not analyzed | $1.2 \times 10^{-3}$/— | 868.02 |
| | Nd + S | 1.50* [4] | 3.5 + 3.5 | 3 + 3 | 205/not analyzed | $3.9 \times 10^{-3}$/— | 868.80 |

[a] A: Dopants. B: Ionic radius[21] (or bond distance, if starred), for the number of coordination indicated in brackets (Å). In cases II, III, and IV the value corresponds to non rare-earth element. C: Critical concentration in the flux defined as 100(maximum doping oxide)/(maximum doping oxide + substituted oxide) (mol %). D: Used concentration defined as 100(used doping oxide)/(used doping oxide + substituted oxide) (mol %). E: Dopant concentration in the crystal (ppm). F: Distribution coefficient defined as $K_{DE} = (DE/(DE + KTP))_{crystal}/(DE/(DE + KTP))_{solution}$ (weight ratio) with DE = RE or Me. G: Cell volume (Å$^3$).

## Experimental Section

**Solutions.** To find out the concentration and temperature regions where RE-doped KTP appears as the highest temperature crystallization phase, already published data on the crystallization regions of undoped KTP phase from the $K_2O-P_2O_5-TiO_2$ system were taken into account.[10,11] Different solution compositions in and around this crystallization region were investigated when part of $TiO_2$ was substituted by $RE_2O_3$ (RE = Nd, Ho, Er, Tm, and Yb) or by $Tb_4O_7$. All these preliminary investigations were made in a vertical cylindrical resistance furnace controlled by a Eurotherm 818P controller/programmer, using small conical crucibles of 20−30 mm in diameter and 30 mm high, filled with about 25 g of solution. Initial reagents of $K_2CO_3$, $NH_4H_2PO_4$, $TiO_2$, and $RE_2O_3$ or $Tb_4O_7$ (p.a.) were used in the desired proportion and mixed before being put into the crucible.

The mixed reagents were decomposed by heating them to 950 °C. They were held at this temperature until the bubble process ($NH_3$, $H_2O$, $CO_2$) was completely finished. The solution was homogenized by maintaining the temperature at 1000 °C for 3−5 h. After that, a 15 mm diameter Pt disk, rotating at 40 rpm, was dropped into the center of the solution free surface. Then, the solution temperature was reduced step by step (∼10 °C/30 min) observing the rotating Pt disk for the appearance of crystals, which subsequently were grown for several hours at a constant temperature. After cooling to room temperature and cleaning with boiling $HNO_3$, the crystals were identified by X-ray powder diffraction, and the crystallization regions of the RE-doped KTP phase were obtained. Independent of the fact that the phase boundaries for the different REs at different initial concentrations were not exactly equally located, a common KTP crystallization region was observed.

One point located in the region with a $K_2O/P_2O_5$ molar ratio of 60/40 and a $(K_2O + P_2O_5)/(TiO_2 + RE\ oxide)$ molar ratio of 83/17 was chosen as a basic composition for the following experiences. At this point, a new series of spontaneous crystallizations in the aforementioned conditions was made in order to obtain the highest (critical) concentration of the RE oxides in the initial solution from which the primary crystallization is only the KTP phase. Two kinds of experiments were carried out in this series. In the first one, different REs were used (RE = Nd, Tb, Ho, Er, Tm, and Yb), while in the second one, only Nd was investigated, but in combination with a second dopant ion for KTP (double substitution). The reagents used for the second doping were $Al_2O_3$, $Nb_2O_5$, $Na_2CO_3$, $Rb_2CO_3$, $K_2SO_4$, and $SiO_2$ (p.a.). So, the doping schemes in the solute were

I. $K(Ti_{1-x}RE_x)OPO_4$, RE being Nd, Tb, Ho Er, Tm, or Yb

II. $K(Ti_{1-2x}Nd_xMe_x)OPO_4$, Me being Al or Nb

III. $(K_{1-x}Me_x)(Ti_{1-x}Nd_x)OPO_4$, Me being Rb or Na

IV. $K(Ti_{1-x}Nd_x)O(PO_4)_{1-x}(MeO_4)_x$, Me being S or Si

In this way information was obtained about the critical RE oxide concentration, as well as about the final concentration of the RE elements in the crystal as a function of the RE ionic radius (I) or the charge and the ionic radii of the corresponding Me codopants (II and III). Two anionic substitutions were also considered in order to analyze the variation of the final RE crystal concentration as a function of the anionic size and charge of both phosphate codopants (IV). Some doping details are shown in the first two columns of Table 1.

**X-ray Diffraction and Cell Volumes.** The X-ray powder diffraction technique was used to identify the phase that first crystallizes from all of the compositions investigated. For these measurements, the crystals obtained on the Pt disk were homogeneously ground, and the powder was analyzed using a Siemens D5000 powder diffractometer in a $\theta-\theta$ configuration using Bragg−Brentano geometry. Further details of the diffraction experiments are given in Table 2. The cell volumes were determined using the FULLPROF program[12] and the Rietveld method. The coordinates of the KTP atoms obtained by Solé et al.[13] were used as the starting model for the calculations. A pseudo-Voigt function was selected to describe individual line profiles and the final Rietveld refinement included the following parameters: one zero-point parameter, one scale factor, four background coefficients, three cell parameters, three half-width parameters, one Lorentzian isotropic strain parameter, one profile shape parameter, and two asymmetry parameters. About 400 reflections were used in all cases.

**Dopant Concentration Analyses.** Doped KTP single crystals, obtained using the highest (critical) concentration of dopants (or up to this level), were separated and cleaned. Some of them, free from inclusions, were dissolved to obtain solutions suitable for inductively coupled plasma (ICP) and atomic absorption spectroscopy (AAS) analyses. Jobin Yvon France JY-38 ICPA and PYE UNICAM SP-192 AAS equipment was used to obtain the concentration of the doping elements in the KTP crystals. Special attention was paid to the determination of the most suitable spectral line in order

(10) Iliev, K.; Peshev, P.; Nikolov, V.; Koseva, I. *J. Cryst. Growth* **1990**, *100*, 219.
(11) Iliev, K.; Peshev, P.; Nikolov, V.; Koseva, I. *J. Cryst. Growth* **1990**, *100*, 225.
(12) Rodriguez Carvajal, J. In Collected Abstracts of Powder Diffraction Meeting, Toulouse, France, July 1990.
(13) Solé, R.; Ruiz, X.; Cabré, R.; Gavaldà, Jna.; Aguiló, M.; Díaz, F.; Nikolov, V.; Solans, X. *J. Cryst. Growth* **1996**, *167*, 681.

**Table 2. Details of Powder Diffraction Experiments and FULLPROF Calculations**

| | |
|---|---|
| space group of KTP | $Pna2_1$ |
| $Z$ | 4 |
| $2\theta$ range (deg) | 10−70 |
| step size (deg) | 0.02 |
| step time (s) | 16 |
| no. of fitted parameters | 15 |

to minimize the errors of the analyses.[14]

**Top Seeded Solution Growth (TSSG).** To obtain preliminary information about crystal growth conditions for RE-doped KTP and also to obtain inclusion-free single crystals of a suitable size for optical investigation, two crystal growth series were made by TSSG and slow cooling.

*Series I.* Solutions of 25−30 g were prepared in cylindrical platinum crucibles, 30 mm in diameter and 40 mm high. A vertical resistance furnace, controlled by a Eurotherm 818P controller/programmer, was used. The axial and radial temperature differences in the solutions were 12 and 3 °C, respectively. For these experiments, *c* oriented seeds were fixed acentrically at 10 mm from the center, with *b* in the radial direction of the rotation movement. The rotation velocity was maintained constant at 27 rpm. The temperatures of saturation were determined by observing the dissolution or growth of the seed. During the growth processes the temperature was reduced by 0.4−0.5 °C/h for the first 3−4 °C and by 0.2 °C/h for the next 20−25 °C. After 5−6 days and 25−30 °C of cooling, doped KTP crystals with dimensions between 2 and 11 mm, depending on the direction, were obtained.

*Series II.* Solutions of 90−100 g were prepared in cylindrical platinum crucibles, 50 mm in diameter and 65 mm high. The temperature was controlled using the same type of controller/programmer than in series I. The axial and radial temperature differences were 7 and 3 °C, respectively. The seeds were *b* oriented and fixed acentrically at 15 mm from the center, while *a* was in the radial direction of the rotation movement. The saturation temperature was determined in the same way as in series I. The doped crystals were grown by slow cooling, and the temperature was decreased at an average rate of 2 °C/day. After 8 days, single crystals with dimensions between 2 and 13 mm, depending on the direction, were obtained.

**Optical Absorption.** Optical absorption studies were performed on plates cut perpendicular to the *c* axis using a diamond saw. These plates were oriented by a conventional Laue X-ray diffraction technique and then polished to optical quality using diamond powders with three succesive grain sizes (6, 3, and 1 $\mu$m). The spectra were collected at 4.2 K with a Varian Model 5E spectrophotometer and an Oxford cryostat controlled with a Lake Shore Model DRC91C controller.

## Results and Discussion

**Crystallization Regions of RE Doped KTP.** Figure 1 shows the crystallization region and neighboring phases of undoped KTP according to a previous investigation[11] (dashed line). As an example, the same figure shows the region of doped KTP for 6 mol % $Nd_2O_3$ substituting $TiO_2$ in the solution. It can be observed that the undoped KTP phase has a wide crystallization region, and the neighboring phases in this case are $KPO_3$ and $K_4P_2O_7$ in the region rich in $K_2O$ and poor in $TiO_2$; $K_2Ti_6O_{13}$ in the region poor in $P_2O_5$ and with a medium content of $TiO_2$; $TiO_2$ (rutile) in the region poor in $P_2O_5$ and rich in $TiO_2$, and $KTi_2(PO_4)_3$ in the region in which the quantity of $K_2O$ in the initial solution is low. Comparing this region with the new one when $Nd_2O_3$ is present in the solution, a remarkable difference can be detected. The neodymium-doped KTP phase has a significantly narrower region, and some neighboring phases are new. In the region poor in $P_2O_5$, $K_3Nd(PO_4)_2$ is a neighbor of KTP, and in the region rich in $Nd_2O_3$, $NdPO_4$ appears as a new phase. Moreover, as the mol percent of $Nd_2O_3$ increases, the boundary "$l_2$" (Figure 1) moves to the right and the boundary "$l_3$" moves considerably more to the left, so at 7 mol % of $Nd_2O_3$, the KTP region practically disappears. We can say that in the quaternary system $K_2O-P_2O_5-TiO_2-Nd_2O_3$, the two ternary systems $K_2O-P_2O_5-TiO_2$ and $K_2O-P_2O_5-Nd_2O_3$ are in competition. It seems that the liquidus surface of the latter is at a significantly higher temperature than that of the system with $TiO_2$, and this can be the reason, for small quantities of $Nd_2O_3$, the phases from the $K_2O-P_2O_5-Nd_2O_3$ system crystallize before than those from the $K_2O-P_2O_5-TiO_2$ system. Several of the compositions tested from the system $K_2O-P_2O_5-TiO_2-Nd_2O_3-WO_3$ showed that the presence of $WO_3$ as solvent in the solution does not change the phenomena discussed.[13]

The experiments show that in all the cases of RE doping studied, similar behavior can be observed as far as the location of the concentration regions and the kind of phases are concerned. It is interesting to note that, independent of the kind of RE oxide and its concentration in the solution, if the latter is lower than the critical value in which the KTP phase disappears, the crystallization temperature of the doped KTP is the same for all RE ions and equal to that of undoped KTP for the same composition of the initial solution.

**Critical Concentration of the RE Oxides.** For growing RE-doped KTP crystals, the critical concentration of the rare earth below which it is possible to obtain the KTP phase and above which other phases appear is a very important parameter. These critical rare-earth concentrations were found by performing the same kind of experiments described above for the determination of the KTP crystallization regions. For this purpose, the composition marked on Figure 1 as point "A" was chosen. Below this point, the region is too narrow and above this point, viscosity problems could appear as they did for undoped KTP single-crystal growth. Composition "A" has 17 mol % ($TiO_2$ + RE oxide) and 83 mol % ($K_2O$ + $P_2O_5$) where the molar ratio $K_2O/P_2O_5$ is 60/40. The critical concentrations for every case of RE doping as well as for the cases of double substitution are summarized in Table 1.

As can be seen in Table 1, there are no large differences between the critical concentrations of RE elements. The small deviation from 6 mol % of RE oxide which substitutes $TiO_2$ in the solution (3 mol % for $Tb_4O_7$, which is equivalent as far as the number of RE atoms are concerned) can be explained by a slight difference in the stability of the $REPO_4$ as a phase in competition with the KTP. In all cases of double substitution, the critical concentration of $Nd_2O_3$ is lower than for single substitution. Note that, in the cases of double substitution, the molar ratios of RE and codopant oxide to the substituted oxide in the solution have been taken equal.

**RE Distribution Coefficients and Cell Volumes.** Table 1 also shows the concentration of dopants in the crystals according to the results of ICP and AAS analyses and the cell volumes of the doped KTP single

(14) Daskalova, N.; Velichkov, S.; Slavova, P.; Ivanova, E.; Aleksieva, L. *Spectrochim. Acta B* **1997**, *52*, 257.

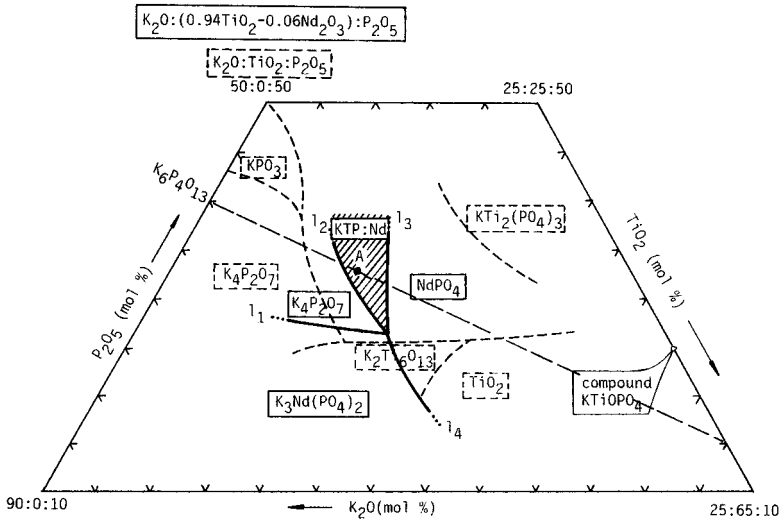


**Figure 1.** Crystallization regions of undoped (dashed line) and Nd-doped KTP (solid line).

crystals. As can be seen, the highest RE concentrations in the crystals change from 52 ppm in the case of Nd to 581 ppm in the case of Yb. These concentrations are at the level at which changes in the ionic conductivity as well as in the absorption spectra may occur.[15] The coefficient of distribution depends on the RE ionic radius and increases by nearly 1 order of magnitude, from $0.6 \times 10^{-3}$ for Nd to $5.8 \times 10^{-3}$ for Yb. These values of the distribution coefficients can be considered normal taking into account the differences in the ionic charges of the $RE^{3+}$ and $Ti^{4+}$ and the large differences in the ionic radii. For a coordination number of six, the ionic radii of the $RE^{3+}$ are in the range 0.983−0.861 Å (see Table 1), while the ionic radius of $Ti^{4+}$ is 0.605 Å.[14]

The cell volumes of KTP single crystals doped with different RE elements are summarized in Table 1. Independent of the rare earth used as dopant, except in the case of Tb, the cell volume of RE-doped KTP tends to be slightly larger than that of undoped KTP. The change in the cell parameters depends on the concentration and the ionic radius of the dopants. Since an increase in the ionic radius causes a decrease in the concentration in the crystal, the final balanced result indicates that there are only slight changes in the cell volume. Figure 2 shows the distribution coefficient of the rare earths, $K_{RE}$, as a function of the ionic radius. It is clear that, as the RE ionic radius increases, the $K_{RE}$ decreases.

The presence of codoping elements generally induces a slight enhancement of the distribution coefficient of Nd ($K_{Nd}$), only the codoping with $Na_2O$ induces a decrease. It can be seen that $K_{Nd}$ approximately doubles by codoping with $Al^{3+}$ or Si, increases 4-fold by codoping with $Rb^+$, 5-fold by codoping with $Nb^{5+}$, and up to 8-fold by codoping with S. It is rather difficult to draw a general conclusion from these results in view of the limited information about the lattice position of the RE dopants. Nevertheless, it seems that to enhance the Nd incorporation to the KTP lattice, codoping should be carried out with an element with ionic radius as near as possible to that to be substituted but with larger charge. For instance, $Nb^{5+}$, which has an ionic radius of 0.64 Å and an ionic charge that is higher than that

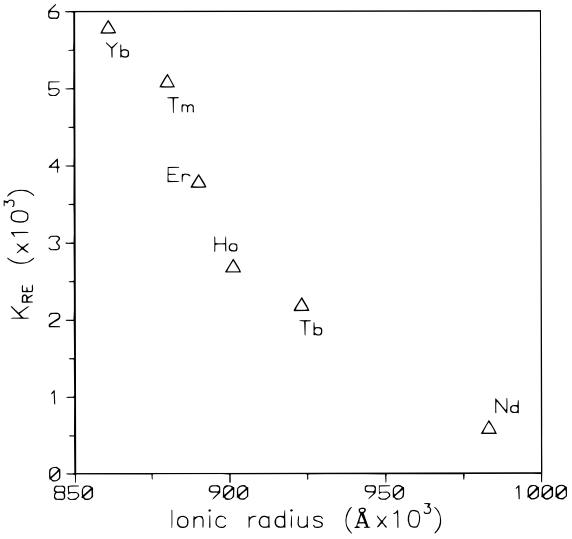


**Figure 2.** Distribution coefficient of rare earth dopants in KTP, $K_{RE}$, as a function of the RE ionic radius.

of $Ti^{4+}$, is more suitable as a codopant than $Al^{3+}$, which has an ionic radius of 0.535 Å and a lower ionic charge. Likewise, their ionic charges being the same, $Rb^+$ (1.61 Å) seems to be a better codopant than $Na^+$ (1.18 Å) when $K^+$ (1.51 Å) has to be substituted. In addition, cosubstitution of the $(PO_4)^{3-}$ group shows that the $(SO_4)^{2-}$ anion is a better codopant than $(SiO_4)^{4-}$ because of its low anionic charge and size. It is important to note that if $Nb_2O_5$ is present in the solution, the critical concentration of $Nd_2O_3$ for which the KTP phase exists is only 1 mol % (see Table 1). Therefore, to increase the $Nd^{3+}$ concentration, the best alternatives for codoping KTP are $Rb^+$ or $(SO_4)^{2-}$.

In the case of double substitution the final cell volume will be related to the two substitution levels. The results (Table 1) show that when the second dopant is a large ion (like $Rb^+$ substituting $K^+$), the cell volume tends to increase and if small ions are used as second dopants ($Al^{3+}$ substituting $Ti^{4+}$ or $Na^+$ substituting $K^+$) the cell volume decreases.

**TSSG of Doped KTP Single Crystals.** As was described in the Experimental Section, two series of RE-doped KTP single-crystal growth were carried out. Significant differences in the growth conditions of

(15) Morris, P. A.; Ferreti, A.; Bierlein, J. D.; Loiacono, G. M. *J. Crystal Growth* **1991**, *109*, 367.

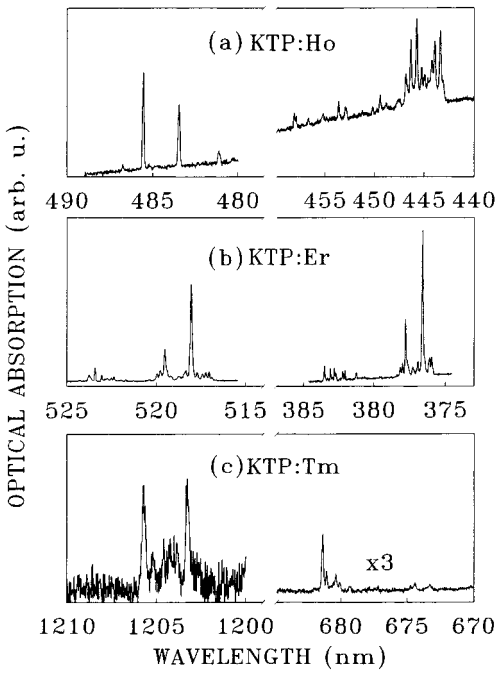


**Figure 3.** The 4.2 K optical absorption spectra of rare-earth-doped KTP crystals. The spectra have been recorded using unpolarized light. (a) KTP:Ho (490−480 nm) $^5I_8 \rightarrow {}^5F_5$ and (460−440 nm) $^5I_8 \rightarrow {}^3K_8 + {}^5F_1 + {}^5G_6$; (b) KTP:Er (525−515 nm) $^4I_{15/2} \rightarrow {}^2H_{11/2}$ and (385−375 nm) $^4I_{15/2} \rightarrow {}^4G_{11/2}$; (c) KTP:Tm (1210−1200 nm) $^3H_6 \rightarrow {}^3H_5$ and (685−670 nm) $^3H_6 \rightarrow {}^3F_3$ transitions.

undoped and doped KTP single crystals were not observed. Practically, the temperature of saturation, the average time of homogenization, and the average rate of growth inclusion-free single crystals were equal. There were no significant differences in the morphology of the crystals.

In all cases, the crystal dimensions in the *a* direction were 3−5 times shorter than in the *b* and *c* ones, and this was independent of the direction of seeding and differences in growth conditions. The differences in size in the *c* and *b* directions were small and depended mainly on the direction of seeding. It is clear that under the growth conditions used, the habit was determined mainly by the solvent composition. The RE incorporation, at least at this low level, scarcely influence the habit.

**Optical Absorption.** The room-temperature optical absorption of rare-earth-doped KTP only shows a weak and broad residual absorption related to the absorption of $Ti^{3+}$ and other lattice defects.[16−18] However, by cooling the samples to 4.2 K, sharp absorption bands overlapping with the absorption background were observed. Figure 3 shows the most intense parts of the unpolarized spectra corresponding to $Ho^{3+}$, $Er^{3+}$, and $Tm^{3+}$ in KTP at 4.2 K. These absorptions are composed of narrow bands arising from the crystal field splitting of the $^{2S+1}L_J$ multiplets.[19] Moreover, additional weaker band sets were observed in other spectral regions. A more detailed description of the optical absorption will be given elsewere.[20] The optical absorption spectra have a strong dichroic character, most of the bands showing their highest intensity when the polarization of light is parallel to the crystal *c* axis.

## Conclusions

The crystallization regions of RE-doped KTP are significantly narrower than that of undoped KTP. Although the phase boundaries are not equally located for all RE studied, a common KTP crystallization region was obtained. For the one point chosen in this region, remarkable differences in the maximum RE concentrations in the solution allowing the crystallization of the KTP phase were not observed.

The distribution coefficient of RE in the obtained crystals ranges from $0.6 \times 10^{-3}$ for Nd to $5.8 \times 10^{-3}$ for Yb and depend on the RE ionic radius. The presence of codoping elements together with Nd doping, generally increases the distribution coefficient of Nd up to 5-fold by codoping with $Nb^{5+}$ and up to 8-fold in the S case.

No significant differences in the growth conditions of undoped and RE-doped single crystals by TSSG technique were observed. The saturation temperature, the homogenization time, the average rate of growth inclusion-free single crystals were very similar. Independent of the direction of seeding, the crystal size along the *a* direction was significant smaller than along the *b* and *c* directions.

Optical absorption spectra of RE-doped KTP at 4.2 K show sharp absorption bands overlapping with the absorption background. These absorptions have a strong dichroic character.

**Acknowledgment.** This work has been supported by CICyT under project TIC96-1039 and by CIRIT under Project 1995SGR 00073. V.N. would also like to acknowledge the financial support received from the Spanish Government (SAB95-0183).

CM960644Z

(16) Roelofs, M. G. *J. Appl. Phys.* **1989**, *65*, 4976.
(17) Martín, M. J.; Bravo, D.; Solé, R.; Díaz, F.; López F. J.; Zaldo, C. *J. Appl. Phys.* **1994**, *76*, 7510.
(18) Scripsick, M. P.; Loiacono, D. N.; Rottenberg, J.; Groellner, S. H.; Halliburton, L. E.; Hopkins, F. K. *Appl. Phys. Lett.* **1995**, *66*, 3428.
(19) Henderson, B.; Imbursch, G. F. In *Optical Spectroscopy of Inorganic Solids*; Clarendon Press: Oxford, 1989; Chapter 8.
(20) Zaldo, C.; Martín, M. J.; Solé, R.; Aguiló, M.; Díaz, F.; Roura, P.; López de Miguel, M. *Opt. Mater.*, submitted.
(21) Shannon, R. D. *Acta Crystallogr.* **1976**, *A32*, 751.